Article

Cell
PRESS

Rheb Regulates Mitophagy Induced by Mitochondrial Energetic Status

Su Melser,[1,6] Etienne Hébert Chatelain,[2,6,7] Julie Lavie,[1,6,7] Walid Mahfouf,[5,6] Caroline Jose,[1,6] Emilie Obre,[1,6]
Susan Goorden,[3] Muriel Priault,[4,6] Ype Elgersma,[3] Hamid Reza Rezvani,[5,6] Rodrigue Rossignol,[1,6]
and Giovanni Bénard[2,6,*]

[1]EA4576, Maladies Rares: Génétique et Métabolisme, 33000 Bordeaux Cedex, France
[2]INSERM U862, Neurocentre Magendie, Physiopathologie de la plasticité neuronale, Endocannabinoids and Neuroadaptation, 33076 Bordeaux, France
[3]Department of Neuroscience, Erasmus University Medical Centre, 3015 Rotterdam, The Netherlands
[4]CNRS IBGC UMR 5095, 33076 Bordeaux, France
[5]INSERM U1035, 33076 Bordeaux, France
[6]Université Victor Segalen-Bordeaux 2, 146 Rue Léo-Saignat, 33076 Bordeaux Cedex, France
[7]These authors contributed equally to this work
*Correspondence: giovanni.benard@inserm.fr
http://dx.doi.org/10.1016/j.cmet.2013.03.014

SUMMARY

Mitophagy has been recently described as a mechanism of elimination of damaged organelles. Although the regulation of the amount of mitochondria is a core issue concerning cellular energy homeostasis, the relationship between mitochondrial degradation and energetic activity has not yet been considered. Here, we report that the stimulation of mitochondrial oxidative phosphorylation enhances mitochondrial renewal by increasing its degradation rate. Upon high oxidative phosphorylation activity, we found that the small GTPase Rheb is recruited to the mitochondrial outer membrane. This mitochondrial localization of Rheb promotes mitophagy through a physical interaction with the mitochondrial autophagic receptor Nix and the autophagosomal protein LC3-II. Thus, Rheb-dependent mitophagy contributes to the maintenance of optimal mitochondrial energy production. Our data suggest that mitochondrial degradation contributes to a bulk renewal of the organelle in order to prevent mitochondrial aging and to maintain the efficiency of oxidative phosphorylation.

INTRODUCTION

The regulation of mitochondrial content is essential for cellular energetic homeostasis, and this regulation is finely tuned according to cellular energy demand and supply. The cellular mitochondrial content is determined by two complex mechanisms: mitochondrial biogenesis and degradation. Mitochondrial biogenesis has been thoroughly investigated, and its importance in terms of energy homeostasis is well established (Scarpulla, 2011). In contrast, the link between bioenergetics and mitochondrial degradation remains unclear.

The degradation of cytosolic components such as organelles can occur through autophagy. Mitophagy is a specific form of autophagy in which mitochondria are specifically targeted for autophagic degradation by the lysosomes (Lemasters, 2005). Three distinct mechanisms of mitophagy have been characterized in the last decade (Youle and Narendra, 2011). The first mechanism has been elucidated in yeast and implicates the mitochondrial protein Atg32 as the mitochondrial receptor for the vacuole targeting of mitochondria to mitophagy. This mechanism is regulated by another mitochondria protein, Uth1 (Kissová et al., 2004; Okamoto et al., 2009). The second mitophagic mechanism has been observed during erythrocyte maturation (Sandoval et al., 2008). This mechanism involves the outer mitochondrial membrane receptor Nix (or Bnip3l) and autophagosome-associated protein LC3 (Novak et al., 2010). The third mechanism involves the Parkinson's disease-related proteins Pink and Parkin (Narendra et al., 2008). Parkin is recruited to the mitochondria when the mitochondrial membrane potential ($\Delta\Psi$) is abrogated by uncoupling, thereby promoting mitophagy (Narendra et al., 2008). Although these mechanisms of mitophagy represent significant advances in our understanding of mitochondrial turnover, the two mitophagic mechanisms described in mammalian cells appear to be restricted to specific physiological conditions. The Pink/Parkin pathway facilitates the clearance of damaged mitochondria after acute stress, whereas mitophagy in reticulocytes is restricted to a specific developmental stage. Yet early studies have proposed the existence of a basal degradation mechanism that contributes to mitochondrial turnover. It has been shown that mitochondria may be completely renewed within 14 days in different tissues and cell types (Huemer et al., 1971; Menzies and Gold, 1971). This renewal requires both mitochondrial biogenesis and degradation. However, the specific mechanism of degradation that participates in the turnover remains to be determined. The cellular mitochondrial energetic status elicits a powerful control over major mitochondrial processes, such as mitochondrial dynamics (Benard et al., 2007), mitochondrial biogenesis (Scarpulla, 2008), and calcium signaling (Bianchi et al., 2004). Thus, mitochondrial bioenergetics may also be linked to mitophagy, and several
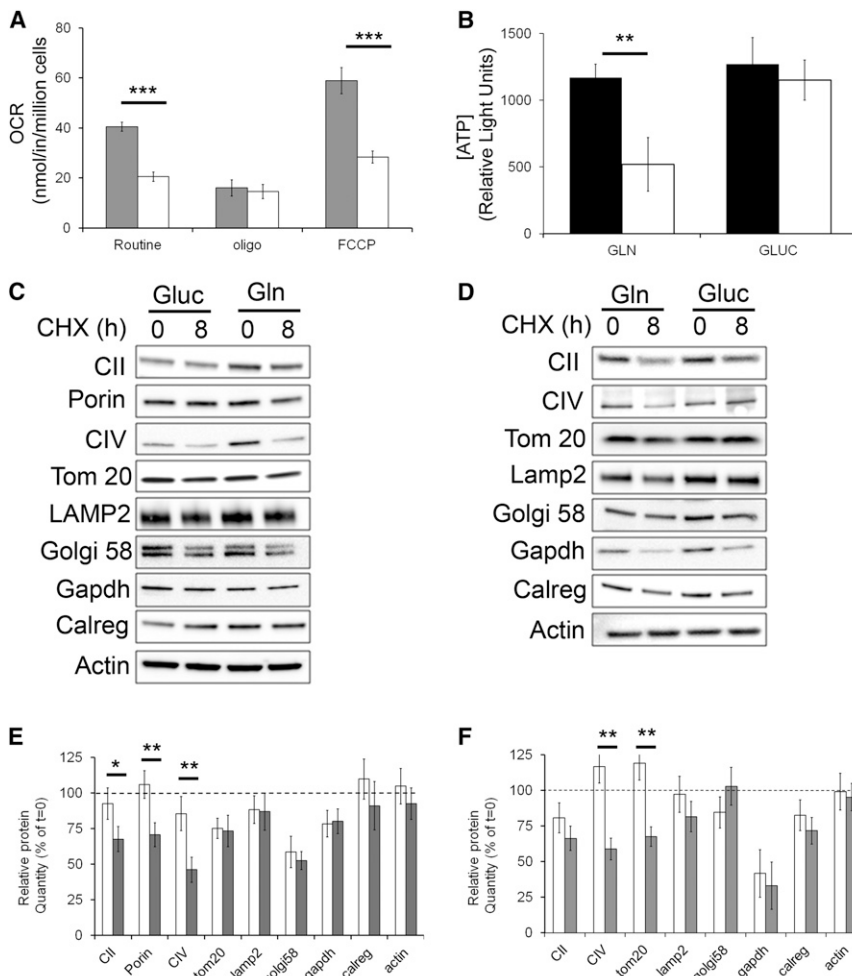
Figure 1. Increased Oxidative Phosphorylation Activity Promotes Mitochondrial Degradation

(A) OCR at routine, noncoupled (oligomycin) and maximal respiration (FCCP) rates measured in HeLa cells grown in glutamine (gray bars) or glucose (white bars) conditions (n = 5).

(B) The total ATP content (black bars) and rotenone-sensitive ATP synthesis (white bars) quantified in cells grown under oxidative (Gln) and glycolytic (Gluc) conditions (n = 4).

(C and D) Protein degradation rates measured in HeLa cells (C) or HSMM (D) grown under oxidative and glycolytic conditions at 0 and 8 hr of treatment with 10 μg/ml CHX. Level of the mitochondrial proteins was analyzed using antibodies against SDHA subunit of complex II (CII), ATP synthase (CV), porin, and Tom20. Golgi apparatus, cytosol, lysosomes, and endoplasmic reticulum were analyzed using Golgi58, Gapdh, Lamp2, and calregulin (calreg) antibodies.

(E and F) Bars are the relative quantification of protein level after 8 hr CHX treatment as shown in (C) and (D) performed on HeLa cells (E) or HSMM (F). White bars are in glucose, and gray bars are in glutamine condition. Values are percentage of respective protein amount at t = 0 (n = 3). Dashed line represents value at t = 0 and normalized to 100% for each protein. *p < 0.05, **p < 0.01, ***p < 0.001 of Gln versus Gluc. Data are presented as mean ± SEM.

studies have identified a relationship between mitophagy and mitochondrial bioenergetic parameters using either pharmacological treatments (Chen et al., 2007; Jin et al., 2010; Narendra et al., 2008) or oxidative phosphorylation (OXPHOS) yeast mutants (Graef and Nunnari, 2011; Priault et al., 2005). Nevertheless, the link between mitochondrial energetic activity and a physiological degradation of mitochondria is still unknown.

In this study, we demonstrated that the stimulation of mitochondrial energy metabolism can regulate mitophagy. We present molecular evidence showing that the small GTPase Rheb (Ras homolog enriched in brain protein) is recruited to the mitochondrial outer membrane upon high OXPHOS activity and regulates mitochondrial energetic status-induced mitophagy. We propose that Rheb participates in the regulation of the renewal of mitochondria to maintain a constant efficiency of mitochondrial energy production.

RESULTS

Stimulation of Oxidative Phosphorylation Enhances Mitochondrial Degradation

To better understand the link between mitochondrial activity and mitochondrial degradation, we analyzed mitochondrial degradation during conditions of high and low OXPHOS activity. To increase this activity, we switched HeLa cells from media containing glucose and no glutamine to glucose-free media supplemented with glutamine, as previously reported (Reitzer et al., 1979; Rossignol et al., 2004; Weinberg et al., 2010). In the same way, human primary skeletal muscle myoblasts (HSMMs) were cultured in the presence or absence of glutamine to have, respectively, low or high OXPHOS activity. Under glutamine-supplemented conditions, HeLa cells displayed a 2-fold increase in the routine oxygen consumption rate (OCR) compared to the cells grown in the presence of glucose only (Figure 1A). The noncoupled OCR induced by the addition of oligomycin was not different between both conditions, while the maximal OCR induced by FCCP in oxidative conditions was twice the rate observed in the glycolytic condition (Figure 1A). Similar results showing that glutamine increased mitochondria respiration were obtained for HSMM (see Figure S1A online). Under routine steady state, HeLa cells produced equivalent amounts of ATP irrespective of the presence of glutamine or glucose. However, the cells grown under oxidative conditions exhibited a strong decrease in mitochondrial ATP production when treated with the complex I inhibitor rotenone, whereas the cells grown in glycolytic conditions were insensitive to the drug (Figure 1B). Using different mitochondrial markers, we could exclude the possibility that this raise was not due to an increase of total mitochondrial content but corresponded to a better feeding of energy substrate to the OXPHOS (Figure S1C). Then we examined the
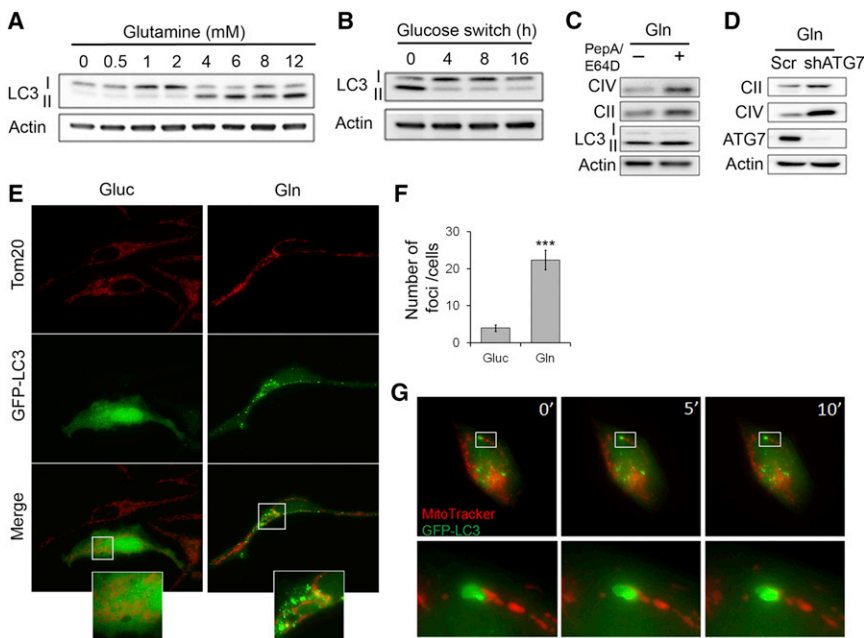
Figure 2. The Activation of Mitochondria Induces Mitophagy

(A) Analysis of LC3-II levels performed on from HeLa cells grown in media with increased glutamine concentrations.

(B) Time course of the reversibility of the glutamine-induced mitophagy assayed after the switch from glutamine to glucose growth media at 0, 4, 8, and 16 hr.

(C and D) Effect of autophagy inhibition on mitochondrial degradation assayed by treatment protease inhibitors, pepstatin/E64D (C) or by ATG7 silencing (D).

(E) GFP-LC3 distribution in HeLa cells under glucose (Gluc) and glutamine (Gln) media. Cells were immunostained with mitochondrial marker Tom20 (red).

(F) Quantification of GFP-LC3 foci per cell from images as shown in (E) (n = 45 cells per condition, ***p < 0.001).

(G) Time course imaging of mitophagy in live cells expressing GFP-LC3 (green) and stained with Mitotracker Red (red) at 4 hr after switching from glucose to glutamine. Data are presented as mean ± SEM.

rate of protein degradation by treating both HeLa and HSMM cells with the protein synthesis inhibitor, cycloheximide (CHX). As a result, cells with high OXPHOS activity (grown in glutamine media) revealed a higher rate of mitochondrial protein degradation compared to low OXPHOS activity (cells grown in glucose). Impact of CHX treatment on protein levels of other cellular compartments such as endoplasmic reticulum (calregulin), Golgi (Golgi-58), lysosome (Lamp2), or cytosol (Actin, Gapdh) were independent of energetic conditions and cell types (Figures 1C–1F). This suggests that solely mitochondrial protein degradation rate is impacted by OXPHOS status.

Mitochondrial Energetic Status Drives Mitophagy

We hypothesized that this degradation of mitochondrial proteins occurred via mitophagy. Thus, we examined mitophagy using a combination of microscopy, immunoblot, and pharmacological inhibition analyses. First, we analyzed the microtubule-associated protein light chain 3 (LC3), which is conjugated to phosphatidylethanolamine (namely, LC3-II) and targeted to autophagic membranes upon the induction of autophagy. In HeLa cells, we observed that a gradual increase of the glutamine concentration promoted the conjugation of LC3-II (Figure 2A) along with an increase in the OXPHOS activity (Figure S1B). Conversely, the switch from oxidative to glycolytic metabolism reversed the LC3-II activation within 4 hr, showing that this phenomenon was inducible and reversible (Figure 2B). We also observed an increase in the number of lysosomes in the cells grown in glutamine compared to glucose (Figures S2A and S2B). To test whether a mitophagic process was responsible for the degradation of mitochondria upon OXPHOS activation, we analyzed the effect of autophagic inhibition on the mitochondrial degradation. The inhibition of autophagic/lysosomal degradation using protease inhibitors pepstatin/E64D or by silencing the autophagic protein 7 (ATG7) hampered mitochondrial degradation induced in glutamine condition (Figures 2C and 2D). The same results

were obtained using other autophagic inhibitors (Figures S2C and S2D). Imaging of cells expressing GFP-LC3 by immunofluorescence microscopy showed LC3 mainly cytosolic in cells grown in glucose but localized as punctate structures in cells grown in glutamine (Figure 2E). Image analysis revealed that the cells grown in glutamine showed a 4-fold increase in the number of LC3 foci per cell compared to cells grown in glucose (Figure 2F). Furthermore, live imaging of GFP-LC3-transfected cells revealed that the newly formed autophagosomes (green foci) could sequentially tether and engulf the mitochondria in glutamine conditions (Figure 2G and Figure S2E). All together, these data suggested that an increase in OXPHOS activity is accompanied by increased mitophagy.

Mitochondrial production of energy via glutamine is mediated by the TCA cycle after the oxidation of glutamine to α-ketoglutarate. To test whether glutamine triggers mitophagy by stimulating mitochondrial energy metabolism through the TCA cycle, we pharmacologically inhibited or bypassed glutaminolysis and assessed the level of LC3-II. First, cells in glutamine media were supplemented with 7 mM dimethyl α-ketoglutarate (DMKG), a cell-permeable analog of α-ketoglutarate, in order to bypass glutaminolysis. Glucose was also added in the media in order to avoid starvation stress. Under these conditions, the ratio of LC3-II to total LC3 significantly increased from 0.43 ± 0.09 to 0.67 ± 0.13 (Figure 3A). In contrast, the inhibition of glutamine catabolism using 2 mM aminooxyacetic acid (AOAA) inhibited mitochondrial respiration and did not promote LC3 activation, as indicated by the ratio of 0.34 ± 0.07 (Figures 3A and 3B). This indicated that the sole presence of glutamine was not sufficient to promote LC3-II formation but that glutamine oxidation by TCA cycle was required to induce mitophagy. When the inhibition of glutamine catabolism by AOAA was bypassed by the addition of DMKG, mitochondrial respiration was restored, and the level of LC3-II was again increased with a ratio of 0.78 ± 0.16. Therefore, the catabolism of glutamine triggered
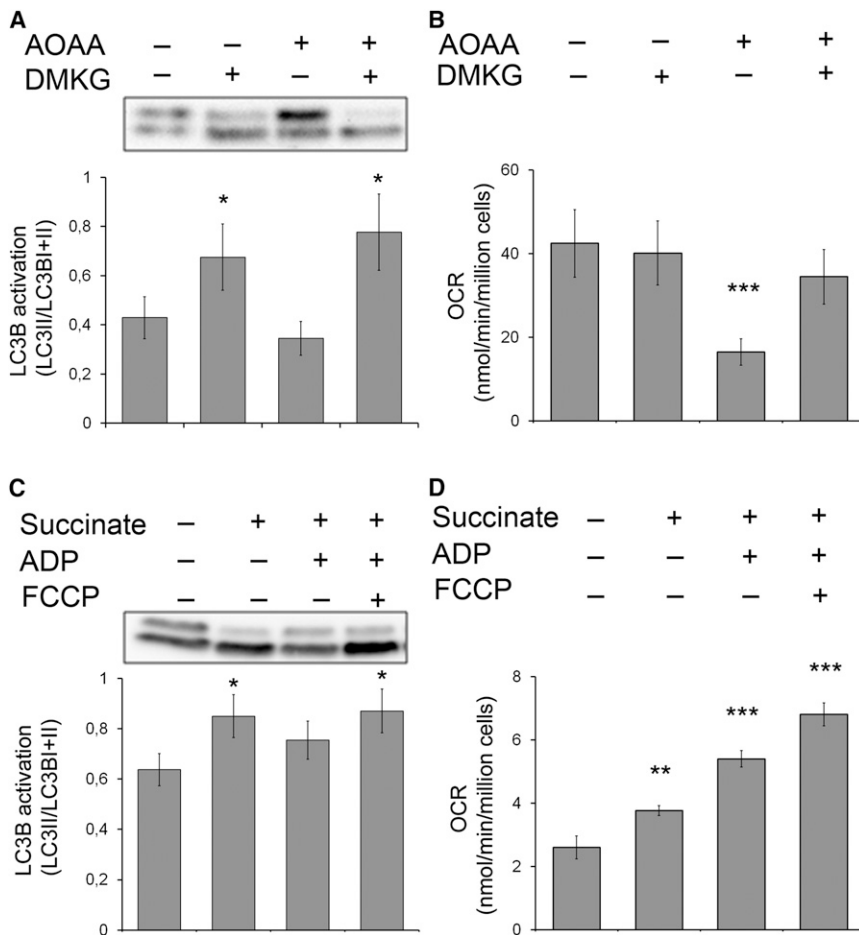
Figure 3. Mitochondrial Energetic Metabolism Drives Mitophagy
(A) Role of glutamine catabolism in the activation of mitophagy. HeLa cells were cultured in the presence of 4 mM glutamine/1 mg/ml glucose and treated with 2 mM AOAA and/or 7 mM DMKG for 24 hr.
(B) OCR associated to AOAA and DMKG treatment.
(C) Direct effect of mitochondrial respiration on LC3 conversion performed on digitonin-permeabilized cells.
(D) Respiration on permeabilized HeLa cells was stimulated with the addition of succinate, ADP and FCCP. *p < 0.05, **p < 0.01, and ***p < 0.001 (n = 3). Data are presented as mean ± SEM.

the conjugation of LC3-II, which is the step required for mitophagy to proceed. Then, cells were placed into an oxygraph chamber and permeabilized with digitonin, and the respiration was stimulated with sequential addition of succinate, ADP and FCCP. Cells were collected, and the conversion of LC3 was analyzed (Figure 3C). The results show that the level of LC3-II increased relative to the permeabilized control cells as the respiratory chain was stimulated with succinate. The corresponding mitochondrial respiration is reported in Figure 3D. Further increase of the mitochondrial respiration either by stimulation of ATP synthesis with ADP or by uncoupling with FCCP did not produce any further significant increase of LC3-II (Figure 3C). Taken together, these results demonstrated that a high mitochondrial respiratory chain activity elicits a direct regulatory effect on mitophagy.

Rheb Participates in Mitochondrial Energetic Status-Induced Mitophagy

To further study the mechanism underlying the mitochondrial energetic status-induced mitophagy, we analyzed the mRNA expression of several autophagy- or mitophagy-related genes after switching the cells from oxidative to glycolytic conditions. As expected, the expression levels of the essential autophagic genes ATG9 and ATG12, as well as the mitochondrial mitophagic receptor Nix, were decreased under glycolytic conditions relative to high OXPHOS conditions. Interestingly, we also found that the expression of Rheb decreased to 50% when the cells were switched to glycolytic conditions (Figure S3A). To test whether Rheb participated in the regulation of mitochondrial energetics-induced mitophagy, we analyzed the impact of ectopic expression of myc-tagged Rheb (Myc-Rheb). As shown in Figure 4A, the expression of Rheb in cells grown in glutamine decreased the overall amount of mitochondria relative to control-transfected cells, as determined by flow-cytometric analysis of cells stained with Mitotracker. Furthermore, the gradual increase in the transient expression of Rheb over 48 hr in cells grown either in glutamine or glucose revealed that Rheb overexpression readily induced the activation of LC3 (Figure 4B). Likewise, we observed a specific reduction in mitochondrial protein levels in both oxidative and glycolytic cells concomitant with the increase of Rheb expression (Figure 4B). Notably, the expression of Rheb was sufficient to induce mitophagy during glycolytic conditions. We observed the same activation of LC3 and specific decrease of mitochondrial protein content in HSMM (Figure 4C). Rheb involvement in mitophagy was further confirmed by microscopy in HeLa cell expressing GFP-LC3, which showed that Rheb expression alone induced the formation of autophagosomes that partially colocalized with mitochondria in glucose-grown cells (Figure 4D). The overexpression of Rheb induced also the intracellular conversion of endogenous LC3 to LC3-II which colocalized with mitochondria (Figure S3B). Inhibition of protein degradation with the protease inhibitors pepstatin A and E64D blocked autophagic degradation (Figure 4E) and hampered mitochondrial degradation (Figure S3C). In the same manner, blockade of autophagic machinery by ATG7 silencing hampered mitochondrial degradation induced by Rheb (Figure 4F). Interestingly, we observed a strong accumulation of Rheb when ATG7 was silenced, suggesting that Rheb is degraded during this mitophagic process. As shown in Figure 4G, the shRNA-mediated downregulation of Rheb specifically induced strong accumulation of mitochondria in HeLa cells. Using conditional knockout mice, we found that
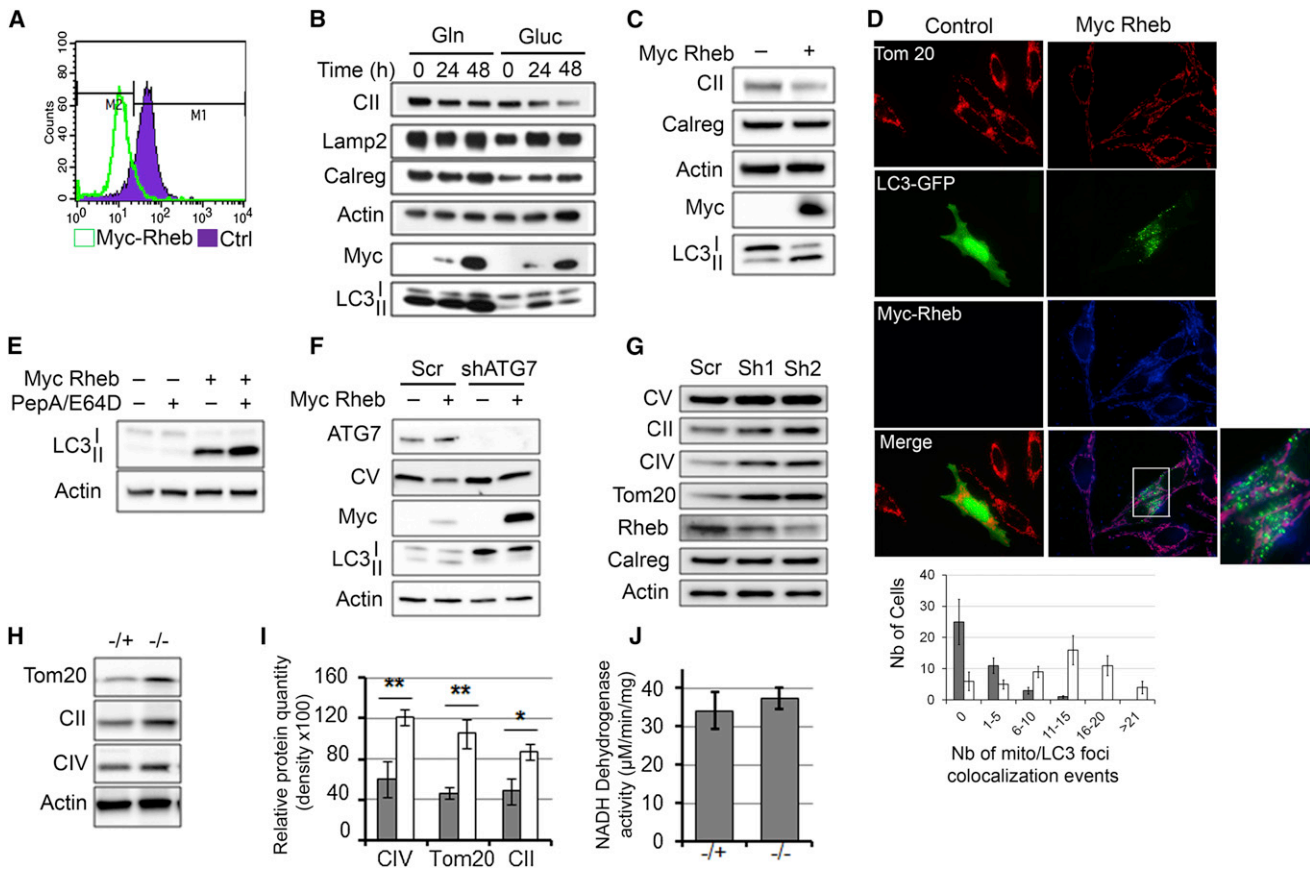
Figure 4. Rheb Induces Mitochondrial Degradation

(A) Analysis of mitochondrial mass by flow cytometry in HeLa cells stained with mitotracker overexpressing Myc-Rheb (green) compared to control transfected cells (purple).

(B) The mitochondrial protein content measured at 0, 24, and 48 hr after transfection with Myc-Rheb in glutamine (Gln) or glucose (Gluc).

(C) Induction of mitochondrial degradation and LC3 conjugation in HSMM cells upon Myc-Rheb overexpression in glycolityc conditions.

(D) Induction of autophagosomes analyzed in cells expressing GFP-LC3 (green) and transfected with Myc-Rheb (blue). Mitochondria were immunostained for Tom20. Bottom graphs represent the number of colocalized LC3 foci and mitochondrial in control (gray bars) and in Rheb-overexpressed cell (white bars) (n > 40 cells).

(E and F) Effect of pepstatin/E64D treatment (E) and ATG7 silencing (F) on LC3 conjugation and mitochondrial protein content.

(G) Effect of Rheb silencing (sh1 and sh2) on mitochondrial degradation respective to control (scramble).

(H) Mitochondrial content in liver of Rheb conditional knockout mouse (−/−) compared to heterozygote (−/+).

(I) Quantification of mitochondrial protein as performed from liver (n = 3–4 animals, $*p < 0.05$, $**p < 0.01$).

(J) NADH dehydrogenase activity in liver of Rheb conditional knockout (−/−) and heterozygote (−/+) mice (n = 3–4 animals). Data are presented as mean ± SEM.

absence of Rheb in liver induced a 2-fold increase of mitochondrial proteins (Figures 4H and 4I). However, OXPHOS activity (namely, NADH dehydrogenase activity) was not increased in the conditional knockout, indicating that this accumulation is dysfunctional (Figure 4J). All together, these findings indicate that Rheb elicits a potent control on mitophagy.

Rheb Is Recruited to the Mitochondrial Outer Membrane

Like several other Ras homologs, Rheb is farnesylated at a C-terminal CAAX domain, and this posttranslational modification anchors the protein to various endomembranes. Interestingly, Rheb has been suggested to be recruited to mitochondria (Ma et al., 2008). To determine whether Rheb is recruited to mitochondria during mitochondrial energetic status-induced mitoph-

agy, we first analyzed its cellular distribution using a whole-cell fractionation method. As shown in Figure 5A, endogenous Rheb was present within the cytosolic fractions (fractions 1 and 2), the lysosomal/autophagosomal fractions (fractions 6 and 7), and the heaviest fractions containing mitochondria (fractions 8 and 10). In the HeLa cells grown in the presence of glutamine, immunofluorescence assays confirmed that Myc-Rheb located strongly to mitochondria (Figure 5B), as tested by the Intensity Correlation Analysis method (Li et al., 2004). The intensity correlation quotient (ICQ) scale ranges between −0.5 and 0.5 where 0.5 corresponds to 100% colocalization, and this quotient was 0.42 ± 0.01 between Tom20-stained mitochondria and Myc-Rheb (n > 50 cells). Immunofluorescence also revealed that in 81% of the cells (n = 320 cells) exhibited a mitochondrial
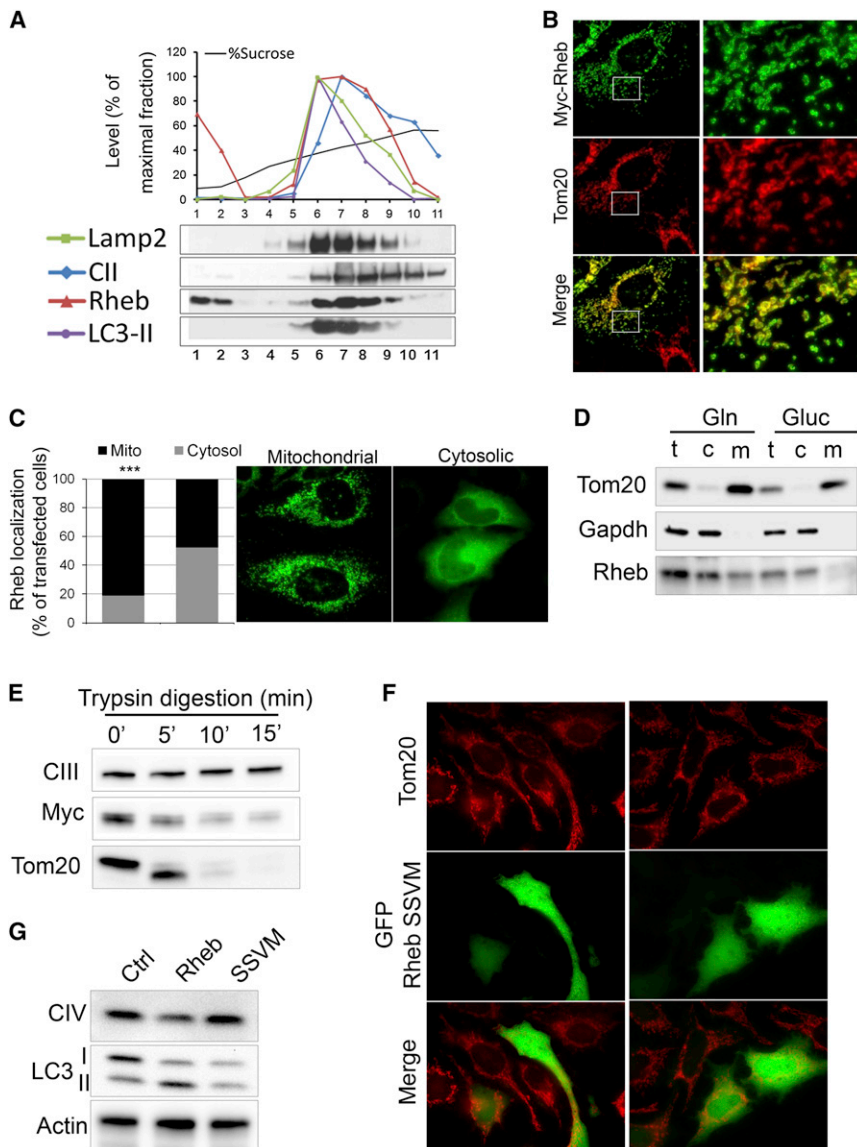
Figure 5. Rheb Locates to Highly Activate Mitochondria

(A) The subcellular localization of endogenous Rheb assessed using sucrose gradient fractionation of oxidative HeLa cells.

(B) Immunofluorescence analysis of Rheb/mitochondria colocalization in HeLa cells transfected with Myc-Rheb (green) and immunostained for mitochondria with Tom20 (red). Asterisk indicates nontransfected cell.

(C) Percentage of cells showing mitochondrial (gray bars) or cytosolic (black bars) distribution of Rheb as shown in the accompanying images.

(D) The subcellular partitioning of endogenous Rheb performed on mitochondrial (m), cytosolic (c), and total cell extract (t) fractions.

(E) The sensitivity of Myc-Rheb to trypsin digestion was assayed on isolated mitochondria. Tom20 and CIII (complex III) were used as respective markers of OMM and IMM.

(F) Analysis of the colocalization of the Rheb CAAX mutant (GFP-Rheb^{SSVM}) and mitochondria (red) analyzed on transfected cells by immunofluorescence.

(G) Effect of SSVM mutant expression on mitochondria protein content and LC3 conjugation analyzed by western blot. ***p < 0.001; p value of mitochondrial localization in glutamine versus glucose. Gln, glutamine; Gluc, glucose.

(Figure 5E). The anchorage of Rheb to the OMM occurs via the farnesyl group, because the cells transfected with a GFP-Rheb-SSVM mutant (i.e., that cannot be farnesylated) did not locate to mitochondria either in glucose (ICQ 0.09 ± 0.02, mito versus GFP-Rheb-SSVM, n > 60 cells) or in glutamine (ICQ 0.11 ± 0.03, n > 60 cells) (Figure 5F). Furthermore, although cells transfected with this mutant displayed LC3 conjugation, mitochondrial degradation was impeded (Figure 5G), showing the importance of the mitochondrial localization of Rheb in this mitophagic mechanism.

In summary, Rheb was preferentially recruited to the OMM in glutamine-grown cells with high OXPHOS activity to promote mitophagy.

Rheb Controls Mitochondrial Bioenergetics-Dependent Mitophagy

To confirm whether Rheb controls mitochondrial energetic status-induced mitophagy, we first assessed the involvement of the mammalian target of rapamycin complex 1 (mTORC1), since Rheb activates mTORC1 (Sancak et al., 2010). The inactivation of mTORC1 during starvation or amino acid deprivation stimulates autophagy (Zoncu et al., 2011), and it has been suggested that mTORC1 is also recruited at the OMM (Desai et al., 2002). As shown in Figure 6A, we found that the activation state of mTORC1 pathways was similar between glycolytic and oxidative conditions. Also, Rheb overexpression further
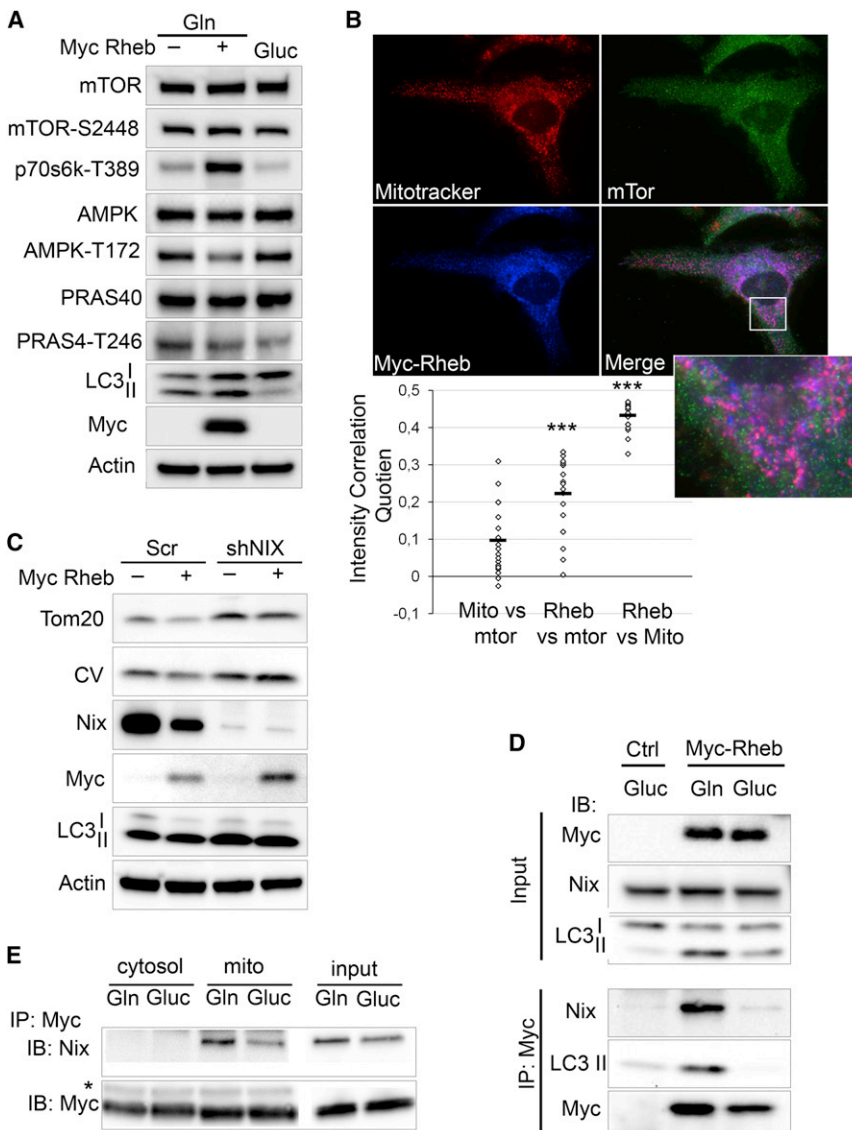
localization of Rheb under oxidative conditions, and this value dropped to 45% of the cells (n = 420 cells) under glycolytic conditions (Figures 5C). We also compared the distribution of endogenous Rheb according to the energetic status of the cells using cell fractionation. Although Rheb was present in mitochondrial fractions in both oxidative (glutamine-grown) and glycolytic (glucose-grown) cells, Rheb was enriched in the mitochondrial fractions isolated from cells grown in oxidative conditions (Figure 5D). The mitochondrial amount of Rheb normalized to Tom20 was 0.72 ± 0.13 in oxidative cells compared to 0.35 ± 0.10 in glycolytic cells (n = 4; p < 0.05). Mitochondrial localization was also obtained by cell fractionation with cells expressing Myc-Rheb (Figure S3D). A trypsin digestion assay was performed using isolated mitochondria from cells expressing Myc-Rheb to estimate the submitochondrial membrane localization of Rheb. The results showed that the Myc tag in the N terminus region of Rheb was digested in the same manner as the OMM protein Tom20, which suggested the OMM localization of Rheb

ing to a 2-fold increase of mitochondria (Figure 6C and Figure S4B), but it did not inhibit LC3 conjugation (Figure 6C). Using BN-PAGE, we also identified a 300 kDa complex containing Nix, Rheb, and LC3 (Figure S4C), and silencing of Rheb modified the profile of Nix oligomerization (Figure S4D). Also, coimmunoprecipitation assays performed on cells expressing Myc-Rheb showed that Rheb physically interacts with both endogenous Nix and LC3 (Figure 6D). This interaction occurred mainly in the mitochondrial fraction of glutamine-grown cells (Figure 6E).We calculated that the ratio of Nix immunoprecipitated from the mitochondrial fraction over the total amount in the input was equal to 1.25 ± 0.25 in glucose compared to 1.80 ± 0.32 in glutamine (n = 3). In summary, Rheb forms a complex with Nix and LC3 that is required for mitochondrial energetic status-induced mitophagy.

Rheb Increases the Efficiency of OXPHOS by Preventing the Accumulation of Damaged Mitochondria

We investigated the effect of Rheb-dependent mitophagy on mitochondrial physiology. Mitophagy has been described as a quality control process that eliminates damaged mitochondria. Under basal conditions, mitochondria from glucose- or glutamine-cultured cells presented neither a collapse of the $\Delta\Psi$, an increase of oxidized proteins, nor a mitochondrial network fragmentation (data not shown). Yet, in oxidative conditions, mitochondria produced slightly more reactive oxygen species (ROS) than in glycolytic conditions and the treatment with the autophagic inhibitor-stimulated ROS production (Figure S5A). In cells that were grown in glutamine media and treated with chloroquine, the mitochondria exhibited high levels of carbonylated proteins (Figures 7A and 7B). The treatment of cells with

activated the mTORC1 pathways, as reflected by the phosphorylation status of different mTORC1 substrates (Figure 6A). These results indicated that Rheb expression activated mTORC1, demonstrating that this signaling pathway is not involved in the mitophagy induced by the stimulation of mitochondrial bioenergetics. The phosphorylation status of mTORC1 was also maintained under AOAA and DMKG treatment (Figure S4A). Moreover, in oxidative conditions, mTORC1 partially colocalized with Rheb (ICQ = 0.22 ± 0.03), but poor mitochondrial localization was observed (ICQ = 0.10 ± 0.03). Rheb and mitochondria strongly colocalized (ICQ = 0.42 ± 0.01) (Figure 6B).

Previous studies showed that Nix is necessary for mitophagy through physical interaction with the autophagosomal protein LC3 (Novak et al., 2010). Thus, we tested if Nix was involved in mitochondrial energetic status-induced mitophagy through an interaction with Rheb. Interestingly, we found that the silencing of Nix hampered the Rheb-induced mitophagy, lead-
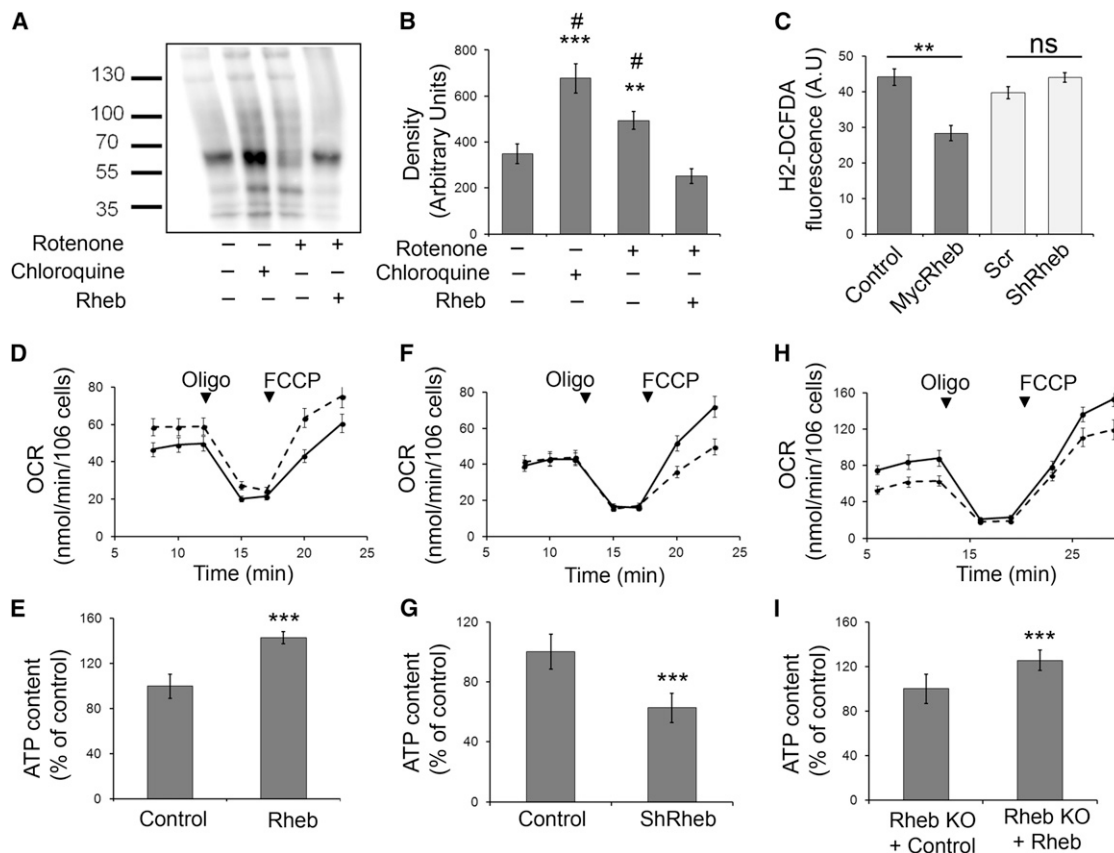
Figure 7. The Positive Impact of Rheb on OXPHOS Activity in Oxidative Conditions

(A) Protein oxidation analysis using the oxyblot method on isolated mitochondria from cells overexpressing Myc-Rheb and treated with chloroquine (10 μM) or rotenone (1 μM). (B) Quantification of Oxyblot assays (n = 3). (C) Quantification of ROS level using DCFDA fluorescent probes in HeLa cells expressing myc-Rheb (gray), shRNA against Rheb (white), and their respective controls. (D, F, and H) Mitochondrial oxygen consumption rates at routine, noncoupled (oligomycin), and maximal (FCCP) steady state in HeLa cells overexpressing Myc-Rheb (D) or in HeLa cell expressing shRNA against Rheb (F), and in MEF Rheb-KO and transfected with human Myc-Rheb (H). OCR were normalized to one million cells (n = 5). (E, G, and I) ATP content in cells expressing Myc-Rheb (E), or shRNA against Rheb (G) and in MEF Rheb-KO and transfected with human Myc-Rheb (I), reported as the percentage of the ATP content in the respective control transfected cells (n = 6–8). ns, nonsignificant; **$p < 0.01$ compared to the control, ***$p < 0.001$ compared to the control, #$p < 0.001$ compared to Rheb-expressing cells. Data are presented as mean ± SEM.

rotenone (complex I inhibitor and ROS inducer) also resulted in an increase in mitochondrial protein carbonylation compared to the control-treated cells, whereas the expression of Rheb reduced the rotenone-induced protein carbonylation by 51.1% ± 12.6% (Figures 7A and 7B). Furthermore, Rheb expression significantly decreased ROS production, while silencing of Rheb had no effect on ROS levels (Figure 7C). These findings strongly suggested that Rheb could ensure the physiological renewal of the mitochondrial pool before the emergence of damaged mitochondria. Therefore, we analyzed whether Rheb had an impact on mitochondrial energy production. We found that the expression of Rheb increased the routine mitochondrial respiration rate by about 25% and enhanced ATP production by 40% (Figures 7D and 7E). Conversely, the silencing of Rheb did not alter the routine respiration, but the maximal oxygen consumption capacity (FCCP-induced OCR) decreased from 72.2 ± 5.6 to 49.8 ± 4.1 nmol/min/million cells (Figure 7F). Also, the loss of Rheb that resulted in an important uncoupling was associated with a decrease in the ATP content (Figure 7G). The downregu-

lation of Rheb and the associated decrease of ATP strongly impeded cellular proliferation in oxidative conditions, but not in glycolytic conditions (Figure S5B). Reconstitution of Rheb-knockout MEFs with human Rheb was sufficient to enhance the routine and maximal OCR and the ATP (Figures 7H and 7I). Taken together, these results indicate that Rheb-dependent mitophagy is a degradation process that facilitates the constant renewal of mitochondria in order to maintain cellular bioenergetic efficiency, likely by preventing the accumulation of damaged mitochondria.

DISCUSSION

In this study, we explored the link between mitophagy and the regulation of mitochondrial energy status. To date, mitophagy has been mainly regarded as an acute degradative process that is triggered by local and severe mitochondrial damages (Narendra et al., 2008) or as part of a developmental process (Sandoval et al., 2008) for the removal of excess mitochondria.

However, evidence suggests that the regulation of mitochondrial mass also occurs routinely under physiological conditions. Here, we report on a mechanism that links the degradation of undamaged mitochondria to the organelle energetic activity. This mechanism involves Rheb, which we found recruited to the OMM. To our knowledge, this is the first such report of a physiologically significant regulatory mitophagy mechanism.

Mitochondrial energy production constantly adapts to cellular energy demands and substrate supply. In the presence of glucose, HeLa cells strongly repress mitochondrial activity, and ATP is produced by glycolysis. Conversely, when these cells are fed with glutamine, mitochondrial energy metabolism is highly active, and the production of cellular ATP occurs via OXPHOS (Rossignol et al., 2004). We exploited this metabolic plasticity to investigate mitochondrial degradation. Several studies have shown that the mitochondrial mass increases in direct proportion to increases in mitochondrial activity (Li et al., 2011; Rossignol et al., 2004). The measurement of mitochondrial biogenesis in these studies readily explains the changes observed in mitochondrial mass. However, the contribution of degradation to mitochondrial mass at steady state remains largely uncharted. Here, we provide several lines of evidence showing that mitophagy is induced when OXPHOS activity increases. First, we demonstrate that an increased rate of mitochondrial energetic activity accompanies increased mitochondrial degradation. Second, we showed that this degradation occurs through the formation of autophagosomes that tether and eliminate mitochondria. Finally, the inhibition of autophagic processes impaired mitochondrial degradation induced by the stimulation of mitochondrial metabolism.

The fact that mitophagy is activated together with an increase in mitochondrial activity is not surprising. Although one might expect that the inhibition of mitophagy is required to preserve the mitochondria content for production of energy, highly active mitochondria are also more sensitive to damage that might lead to the loss of their ability to produce ATP. Wenz et al. proposed that promoting mitochondrial renewal might ameliorate cytochrome c oxidase deficiency (Wenz et al., 2008).

Moreover, the induction of mitophagy may facilitate the elimination of mitochondria that exhibit OXPHOS deficiency (Sterky et al., 2011; Suen et al., 2010). However, in the elevated oxidative conditions that we studied, the mitochondria were healthy and exhibited intact membrane potential, sustained coupled oxygen consumption, and a nonfragmented network. The elevated production of mitochondrial ATP under these conditions was sufficient to sustain normal cell growth. Yet, in conditions of high OXPHOS activity, cells also displayed elevated mitophagy rates. By constantly renewing the pool of mitochondria through high rates of mitophagy and biogenesis, the cell may be able to maintain the full efficiency of the organelle. Induction of mitophagy upon increased mitochondrial energy production may be triggered as a mechanism to sustain the renewal of mitochondria while simultaneously preventing the accumulation of damage that is associated with elevated mitochondrial utilization. Our data support the model in which mitophagy prevents the loss of mitochondrial fitness by a mechanism that prevents, rather than resolves, mitochondrial aging.

During our investigation, we reported a predominant role for Rheb in the mitophagy mechanism induced by mitochondrial bioenergetics. We observed that Rheb expression induced mitophagy, prevented the accumulation of ROS-induced damage, and improved basal and maximal mitochondrial respiration. In contrast, silencing of Rheb inhibited mitophagy, reduced the rates of mitochondria-coupled respiration, and dramatically reduced cellular growth during glutamine growth conditions. Rheb is a small GTPase that is recognized as an important positive regulator of mTORC1 (Inoki et al., 2003; Saucedo et al., 2003). The inhibition of mTORC1 leads to the activation of general autophagic processes. However, we have excluded the involvement of mTORC1 in this mitophagy mechanism for several reasons. First, we showed that mTORC1 is not inhibited during either oxidative or glycolytic growth conditions. Second, the overexpression of Rheb is known to activate mTORC1, and in such cases, the autophagic processes should be inhibited. However, the ectopic expression of Rheb led to enhanced mitochondrial bioenergetic status-induced mitophagy. Finally, the lack of amino acids, growth factors, or ATP can drive autophagy (Zoncu et al., 2011), and these factors were not deficient in our experimental conditions.

Rheb exhibits mTORC1-independent functions (Neuman and Henske, 2011), such as protein quality control (Zhou et al., 2009), cell signaling (Karbowniczek et al., 2006), and vesicle trafficking (Saito et al., 2005). Rheb has previously been suggested to locate to the mitochondria (Ma et al., 2010), where it was proposed to antagonize the mitochondrial proteins, Fkpb38 and Bnip3 (Bai et al., 2007; Li et al., 2007). Rheb can be farnesylated at a C-terminal CAAX domain (Clark et al., 1997), which allows its anchorage to various endomembranes such as lysosomes (Sancak et al., 2010) or Golgi (Takahashi et al., 2005). Here, we found that increased mitochondrial activity results in the anchorage of Rheb to the OMM through its farnesylated moiety, as Rheb CAAX mutant did not locate to mitochondria. The recruitment of Rheb to mitochondria coincided with the activation of mitophagy, as seen by (1) the activation of LC3-II, (2) the formation of autophagosomes, and (3) a specific decrease of mitochondrial proteins and mass. Moreover, silencing of Rheb was sufficient to block mitochondrial degradation.

Our data demonstrate that Rheb physically interacts with Nix. The role of Nix in mitophagy has been previously characterized (Sandoval et al., 2008), and our data showed that its silencing was sufficient to inhibit Rheb-driven mitophagy. We propose that Rheb is recruited to the OMM to facilitate the interaction between Nix and LC3, thus allowing for the engulfment of mitochondria by nascent autophagosomes. As stated above, Rheb can be recruited to several subcellular compartments (Hanker et al., 2010; Ma et al., 2008; Sancak et al., 2010). Although Rheb is strongly recruited to the OMM during conditions of high mitochondrial activity, the signaling mechanism underlying such localization of Rheb remains unknown. Our data show that the direct stimulation of mitochondrial activity by the supplementation of the TCA cycle with an analog of α-ketoglutarate or by the direct feeding of OXPHOS with succinate is sufficient to induce mitophagy. This argues in favor of a mitochondria-specific pathway that triggers mitophagy, although the specific mitochondrial signal that activates mitochondrial degradation remains to be determined. Interestingly, Nix and its partner Bnip3 are sensitive to low oxygen levels (Bellot et al., 2009; Li et al., 2007). During oxidative conditions, the rate of mitochondrial

oxygen consumption is increased, which may generate local hypoxia, and the potential link between Rheb and hypoxia has been previously described by Li et al. (Li et al., 2007). So it is possible that the mitochondrial recruitment of Rheb is mediated by the activation of Nix due to such mitochondrial local hypoxia.

Haynes et al. recently identified Rheb as one of the four positive hits in a genome-wide RNAi-based screen in *C. elegans* regarding mitochondrial protein quality control, although the authors did not further investigate the molecular mechanism involving Rheb (Haynes et al., 2007) or its impact on mitochondrial functions. In this study, our data illustrate the physiological relevance of Rheb on mitochondrial activity and cellular growth. We reported that the silencing of Rheb dramatically impaired cellular growth when the cells were cultured in oxidative but not glycolytic conditions. We found that Rheb enhanced OXPHOS activity by preventing the accumulation of mitochondrial damage. These data support the concept that Rheb function is essential when mitochondrial metabolism is highly required for cellular energy homeostasis. The importance of Rheb has been already highlighted in mouse models, as Rheb-KO mice are nonviable (Goorden et al., 2011), but the role played by Rheb-induced mitophagy remains to be evaluated in these KO mice. Interestingly, we showed that Rheb knockdown led to a strong accumulation of mitochondria in liver, and this increase is not associated with a rise of mitochondrial activity, suggesting a pathological situation.

In conclusion, by establishing a link between mitochondrial bioenergetics and mitophagy, Rheb ensures the efficiency of mitochondrial energy production. This mechanism provides fundamental implications for mitochondrial physiology.

EXPERIMENTAL PROCEDURES

Materials

Choroquine, E64D/Pepstatin A, oligomycin, FCCP, DMKG, and AOAA were purchased from Sigma Aldrich. Plasmids constructs used in this study were from Addgene (see Table S1). The Myc-Rheb construct was a kind gift from Kun-Liang Guan. Rheb shRNAs were pursached from Sigma Mission RNA, and sequences are listed Table S2.

Cell Culture, Transfection, and Pharmacology

HeLa and MEF cells were cultured under 5% CO_2 at 37°C either in glucose media consisting of DMEM medium supplemented with 25 mM glucose or in DMEM glucose-free medium supplemented with 4 mM glutamine and 10 mM galactose. Both media were supplemented with 10% fetal bovine serum, 1 mM sodium pyruvate, MEM nonessential amino acids, and 100 U/ml penicillin/streptomycin. HSMMs were cultured according to the manufacturer's protocol (Lonza), but glutamine was either not present in the media or was added at 4 mM. The cells were transfected using FugeneHD (Roche). Gradual activation of LC3 with increase of glutamine concentration was performed in galactose media supplemented with various concentration of glutamine, but we added 1 mg/ml glucose in order to avoid starvation at 0 mM glutamine. DMKG was used at 7 mM and AOAA at 2 mM for 24 hr.

Sucrose Gradient Experiments and Cell Fractionation

For isopycnic separation, total fresh HeLa extracts were loaded onto the top of 10%–60% (w/v) sucrose gradients and centrifuged for 4 hr at 100,000 g. Fractions of 1 ml were collected, diluted with buffer without sucrose (5 mM $MgCl_2$, 20 mM HEPES [pH 7.4], 10 mM KCl, 1 mM EDTA), and pelleted.

For subcellular fractionation, cells were harvested in isotonic mitochondrial buffer supplemented with the protease inhibitor (Roche) and homogenized for 20 strokes with a 25-gauge syringe. The samples were centrifuged at 500 × g for 5 min at 4°C. The supernatant was centrifuged at 10,000 × g for 15 min at

4°C to obtain the heavy membrane pellet enriched in mitochondria, and the resulting supernatant was stored as the cytosolic fraction. The pellets were resuspended and subjected to an additional cycle of centrifugation. The final pellets were resuspended in 2× laemmli buffer.

Western Blot Analysis and Immunoprecipitation

Samples were analyzed by western blot analysis using conventional methods. Proteins were detected using specific antibodies against Rheb and LC3 (Cell Signaling), Tom20, Lamp2 and calregulin (SantaCruz), Gapdh, Golgi 58, OXPHOS and ANT (Abcam), and Myc-tag (Roche). β-actin (Sigma-Aldrich) was used as the loading control.

Protein oxidation was evaluated using the Oxyblot kit (Millipore) according to the manufacturer's protocols.

For the coimmunoprecipitation assays, the total, mitochondrial, and cytosolic fractions were diluted in lysis buffer (1% Triton X-100, 50 mM Tris [pH 7.4], 150 mM NaCl, 10 mM EDTA, and protease inhibitors). Each fraction was incubated for 4 hr with anti-Myc agarose beads at 4°C. Beads were watched several times with TBS-Tween 20 0.05%. Proteins were eluted with 2× laemmli sample buffer.

Immunofluorescence

Immunofluorescences were performed according to classical protocols using 4% paraformaldehyde fixation and Triton X-100 permeabilization. Images were acquired using a AxioZision microscope (Zeiss) with a 63× objective. Z sections (interval of 0.2 μm) covering the entire depth of the cell were acquired. Live-cell imaging experiments were performed in chambers containing 5% CO_2 and maintained at 37°C. Colocalization analyses were performed using the Intensity Correlation Analysis plug-in from MacBiophotonics ImageJ software.

Respiration and ROS Assays

Mitochondrial oxygen consumption assays were performed using the high-resolution respirometry system Oxygraph-2k (Oroboros, Austria). Cellular respiration was measured with 1 × 10^6 cells/ml at 37°C. The endogenous OCR measurements included the following: (1) routine physiological coupled OCR, (2) noncoupled resting OCR after ATPsynthase inhibition with 2 μg/ml oligomycin, and (3) maximal uncoupled OCR as titrated with FCCP (2 μM steps). ROS levels were monitored using the H2-DCFDA probe (Invitrogen) with 1 × 10^6 cells/ml using a fluorometer with excitation at 495 nm and emission recorded between 510 and 550 nm.

Rheb Mice

Mice carrying a floxed ($Rheb^{+/f}$) or knockout Rheb ($Rheb^{+/-}$) allele (Goorden et al., 2011) were crossed at least 12 times into the C57BL/6JOlaHsd background. To create a tamoxifen-inducible *Rheb1* knockout line, floxed *Rheb* ($Rheb^{+/f}$) mice were crossed with floxed *Rheb* ($Rheb^{-/f}$)-CAG-cre/Esr1 transgenic mice (Hayashi and McMahon, 2002) to yield the inducible $Rheb^{f/-}$ CAG-cre/Esr1 and $Rheb1^{f/+}$CAG-cre/Esr1 mutant. Adult (2–3 month) mice were i.p. injected with tamoxifen dissolved in sunflower oil (10 mg/g) for 4 days to induce the gene deletion resulting in $Rheb^{-/-}$ and $Rheb^{+/-}$mice. These mice were sacrificed 17 days following the first injection.

Statistics

All values are the mean ± SEM. The statistics were performed with GraphPad Prism 5 software using an unpaired Student's t test to compare two independent groups or pair for sequential measurements. One-way and two-way ANOVA were performed when comparing different groups.

SUPPLEMENTAL INFORMATION

Supplemental Information includes five figures, two tables, and Supplemental Experimental Procedures and can be found with this article at http://dx.doi.org/10.1016/j.cmet.2013.03.014.

ACKNOWLEDGMENTS

REFERENCES

Bai, X., Ma, D., Liu, A., Shen, X., Wang, Q.J., Liu, Y., and Jiang, Y. (2007). Rheb activates mTOR by antagonizing its endogenous inhibitor, FKBP38. Science 318, 977–980.

Bellot, G., Garcia-Medina, R., Gounon, P., Chiche, J., Roux, D., Pouysségur, J., and Mazure, N.M. (2009). Hypoxia-induced autophagy is mediated through hypoxia-inducible factor induction of BNIP3 and BNIP3L via their BH3 domains. Mol. Cell. Biol. 29, 2570–2581.

Benard, G., Bellance, N., James, D., Parrone, P., Fernandez, H., Letellier, T., and Rossignol, R. (2007). Mitochondrial bioenergetics and structural network organization. J. Cell Sci. 120, 838–848.

Bianchi, K., Rimessi, A., Prandini, A., Szabadkai, G., and Rizzuto, R. (2004). Calcium and mitochondria: mechanisms and functions of a troubled relationship. Biochim. Biophys. Acta 1742, 119–131.

Chen, Y., McMillan-Ward, E., Kong, J., Israels, S.J., and Gibson, S.B. (2007). Mitochondrial electron-transport-chain inhibitors of complexes I and II induce autophagic cell death mediated by reactive oxygen species. J. Cell Sci. 120, 4155–4166.

Clark, G.J., Kinch, M.S., Rogers-Graham, K., Sebti, S.M., Hamilton, A.D., and Der, C.J. (1997). The Ras-related protein Rheb is farnesylated and antagonizes Ras signaling and transformation. J. Biol. Chem. 272, 10608–10615.

Desai, B.N., Myers, B.R., and Schreiber, S.L. (2002). FKBP12-rapamycin-associated protein associates with mitochondria and senses osmotic stress via mitochondrial dysfunction. Proc. Natl. Acad. Sci. USA 99, 4319–4324.

Goorden, S.M., Hoogeveen-Westerveld, M., Cheng, C., van Woerden, G.M., Mozaffari, M., Post, L., Duckers, H.J., Nellist, M., and Elgersma, Y. (2011). Rheb is essential for murine development. Mol. Cell. Biol. 31, 1672–1678.

Graef, M., and Nunnari, J. (2011). Mitochondria regulate autophagy by conserved signalling pathways. EMBO J. 30, 2101–2114.

Hanker, A.B., Mitin, N., Wilder, R.S., Henske, E.P., Tamanoi, F., Cox, A.D., and Der, C.J. (2010). Differential requirement of CAAX-mediated posttranslational processing for Rheb localization and signaling. Oncogene 29, 380–391.

Hayashi, S., and McMahon, A.P. (2002). Efficient recombination in diverse tissues by a tamoxifen-inducible form of Cre: a tool for temporally regulated gene activation/inactivation in the mouse. Dev. Biol. 244, 305–318.

Haynes, C.M., Petrova, K., Benedetti, C., Yang, Y., and Ron, D. (2007). ClpP mediates activation of a mitochondrial unfolded protein response in C. elegans. Dev. Cell 13, 467–480.

Huemer, R.P., Lee, K.D., Reeves, A.E., and Bickert, C. (1971). Mitochondrial studies in senescent mice. II. Specific activity, buoyant density, and turnover of mitochondrial DNA. Exp. Gerontol. 6, 327–334.

Inoki, K., Li, Y., Xu, T., and Guan, K.L. (2003). Rheb GTPase is a direct target of TSC2 GAP activity and regulates mTOR signaling. Genes Dev. 17, 1829–1834.

Jin, S.M., Lazarou, M., Wang, C., Kane, L.A., Narendra, D.P., and Youle, R.J. (2010). Mitochondrial membrane potential regulates PINK1 import and proteolytic destabilization by PARL. J. Cell Biol. 191, 933–942.

Karbowniczek, M., Robertson, G.P., and Henske, E.P. (2006). Rheb inhibits C-raf activity and B-raf/C-raf heterodimerization. J. Biol. Chem. 281, 25447–25456.

Kissová, I., Deffieu, M., Manon, S., and Camougrand, N. (2004). Uth1p is involved in the autophagic degradation of mitochondria. J. Biol. Chem. 279, 39068–39074.

Lemasters, J.J. (2005). Selective mitochondrial autophagy, or mitophagy, as a targeted defense against oxidative stress, mitochondrial dysfunction, and aging. Rejuvenation Res. 8, 3–5.

Li, Q., Lau, A., Morris, T.J., Guo, L., Fordyce, C.B., and Stanley, E.F. (2004). A syntaxin 1, Galpha(o), and N-type calcium channel complex at a presynaptic nerve terminal: analysis by quantitative immunocolocalization. J. Neurosci. 24, 4070–4081.

Li, Y., Wang, Y., Kim, E., Beemiller, P., Wang, C.Y., Swanson, J., You, M., and Guan, K.L. (2007). Bnip3 mediates the hypoxia-induced inhibition on mammalian target of rapamycin by interacting with Rheb. J. Biol. Chem. 282, 35803–35813.

Li, L., Pan, R., Li, R., Niemann, B., Aurich, A.C., Chen, Y., and Rohrbach, S. (2011). Mitochondrial biogenesis and peroxisome proliferator-activated receptor-γ coactivator-1α (PGC-1α) deacetylation by physical activity: intact adipocytokine signaling is required. Diabetes 60, 157–167.

Ma, D., Bai, X., Guo, S., and Jiang, Y. (2008). The switch I region of Rheb is critical for its interaction with FKBP38. J. Biol. Chem. 283, 25963–25970.

Ma, D., Bai, X., Zou, H., Lai, Y., and Jiang, Y. (2010). Rheb GTPase controls apoptosis by regulating interaction of FKBP38 with Bcl-2 and Bcl-XL. J. Biol. Chem. 285, 8621–8627.

Menzies, R.A., and Gold, P.H. (1971). The turnover of mitochondria in a variety of tissues of young adult and aged rats. J. Biol. Chem. 246, 2425–2429.

Narendra, D., Tanaka, A., Suen, D.F., and Youle, R.J. (2008). Parkin is recruited selectively to impaired mitochondria and promotes their autophagy. J. Cell Biol. 183, 795–803.

Neuman, N.A., and Henske, E.P. (2011). Non-canonical functions of the tuberous sclerosis complex-Rheb signalling axis. EMBO Mol. Med. 3, 189–200.

Novak, I., Kirkin, V., McEwan, D.G., Zhang, J., Wild, P., Rozenknop, A., Rogov, V., Löhr, F., Popovic, D., Occhipinti, A., et al. (2010). Nix is a selective autophagy receptor for mitochondrial clearance. EMBO Rep. 11, 45–51.

Okamoto, K., Kondo-Okamoto, N., and Ohsumi, Y. (2009). A landmark protein essential for mitophagy: Atg32 recruits the autophagic machinery to mitochondria. Autophagy 5, 1203–1205.

Priault, M., Salin, B., Schaeffer, J., Vallette, F.M., di Rago, J.P., and Martinou, J.C. (2005). Impairing the bioenergetic status and the biogenesis of mitochondria triggers mitophagy in yeast. Cell Death Differ. 12, 1613–1621.

Reitzer, L.J., Wice, B.M., and Kennell, D. (1979). Evidence that glutamine, not sugar, is the major energy source for cultured HeLa cells. J. Biol. Chem. 254, 2669–2676.

Rossignol, R., Gilkerson, R., Aggeler, R., Yamagata, K., Remington, S.J., and Capaldi, R.A. (2004). Energy substrate modulates mitochondrial structure and oxidative capacity in cancer cells. Cancer Res. 64, 985–993.

Saito, K., Araki, Y., Kontani, K., Nishina, H., and Katada, T. (2005). Novel role of the small GTPase Rheb: its implication in endocytic pathway independent of the activation of mammalian target of rapamycin. J. Biochem. 137, 423–430.

Sancak, Y., Bar-Peled, L., Zoncu, R., Markhard, A.L., Nada, S., and Sabatini, D.M. (2010). Ragulator-Rag complex targets mTORC1 to the lysosomal surface and is necessary for its activation by amino acids. Cell 141, 290–303.

Sandoval, H., Thiagarajan, P., Dasgupta, S.K., Schumacher, A., Prchal, J.T., Chen, M., and Wang, J. (2008). Essential role for Nix in autophagic maturation of erythroid cells. Nature 454, 232–235.

Saucedo, L.J., Gao, X., Chiarelli, D.A., Li, L., Pan, D., and Edgar, B.A. (2003). Rheb promotes cell growth as a component of the insulin/TOR signalling network. Nat. Cell Biol. 5, 566–571.

Scarpulla, R.C. (2008). Transcriptional paradigms in mammalian mitochondrial biogenesis and function. Physiol. Rev. 88, 611–638.

Scarpulla, R.C. (2011). Metabolic control of mitochondrial biogenesis through the PGC-1 family regulatory network. Biochim. Biophys. Acta 1813, 1269–1278.

Sterky, F.H., Lee, S., Wibom, R., Olson, L., and Larsson, N.G. (2011). Impaired mitochondrial transport and Parkin-independent degeneration of respiratory chain-deficient dopamine neurons in vivo. Proc. Natl. Acad. Sci. USA 108, 12937–12942.

Suen, D.F., Narendra, D.P., Tanaka, A., Manfredi, G., and Youle, R.J. (2010). Parkin overexpression selects against a deleterious mtDNA mutation in heteroplasmic cybrid cells. Proc. Natl. Acad. Sci. USA 107, 11835–11840.

Takahashi, K., Nakagawa, M., Young, S.G., and Yamanaka, S. (2005). Differential membrane localization of ERas and Rheb, two Ras-related proteins involved in the phosphatidylinositol 3-kinase/mTOR pathway. J. Biol. Chem. *280*, 32768–32774.

Weinberg, F., Hamanaka, R., Wheaton, W.W., Weinberg, S., Joseph, J., Lopez, M., Kalyanaraman, B., Mutlu, G.M., Budinger, G.R., and Chandel, N.S. (2010). Mitochondrial metabolism and ROS generation are essential for Kras-mediated tumorigenicity. Proc. Natl. Acad. Sci. USA *107*, 8788–8793.

Wenz, T., Diaz, F., Spiegelman, B.M., and Moraes, C.T. (2008). Activation of the PPAR/PGC-1alpha pathway prevents a bioenergetic deficit and effectively improves a mitochondrial myopathy phenotype. Cell Metab. *8*, 249–256.

Youle, R.J., and Narendra, D.P. (2011). Mechanisms of mitophagy. Nat. Rev. Mol. Cell Biol. *12*, 9–14.

Zhou, X., Ikenoue, T., Chen, X., Li, L., Inoki, K., and Guan, K.L. (2009). Rheb controls misfolded protein metabolism by inhibiting aggresome formation and autophagy. Proc. Natl. Acad. Sci. USA *106*, 8923–8928.

Zoncu, R., Bar-Peled, L., Efeyan, A., Wang, S., Sancak, Y., and Sabatini, D.M. (2011). mTORC1 senses lysosomal amino acids through an inside-out mechanism that requires the vacuolar H(+)-ATPase. Science *334*, 678–683.